Correlations and entanglement in quantum critical bilayer and necklace XY models

Johannes Helmes and Stefan Wessel

Phys. Rev. B **92**, 125120 — Published 11 September 2015

DOI: 10.1103/PhysRevB.92.125120

Correlations and entanglement in quantum critical bilayer and necklace XY models

Johannes Helmes[1,2] and Stefan Wessel[1]

[1] *Institut für Theoretische Festkörperphysik, JARA-FIT and JARA-HPC, RWTH Aachen University, 52056 Aachen, Germany*

[2] *Institut für Theoretische Physik, Universität zu Köln, 50937 Köln, Germany*

(Dated: August 25, 2015)

We analyze the critical properties and the entanglement scaling at the quantum critical points of the spin-half XY model on the two-dimensional square-lattice bilayer and necklace lattice, based on quantum Monte Carlo simulations on finite tori and for different subregion shapes. For both models, the finite-size scaling of the transverse staggered spin structure factor is found in accord with a quantum critical point described by the two-component, three-dimensional ϕ^4-theory. The second Rényi entanglement entropy in the absence of corners along the subsystem boundary exhibits area-law scaling in both models, with an area-law prefactor of 0.0674(7) [0.0664(4)] for the bilayer [necklace] model, respectively. Furthermore, the presence of 90° corners leads in both models to an additive logarithmic term. We estimate a contribution of $-0.010(2)$ $[-0.009(2)]$ due to each 90° corner to the logarithmic correction for the bilayer [necklace] model, and compare our findings to recent numerical linked cluster calculations and series expansion results on related models.

I. INTRODUCTION

The study of the entanglement in quantum many-body systems has lead to new insights into the structure of strongly correlated quantum states. One interesting direction of current research in this respect is the identification of universal contributions to the scaling of the bipartite entanglement entropy in quantum many-body systems. For the special case of one-dimensional quantum critical states, described by a conformal field theory, it is well known for example, that the entanglement entropy S asymptotically scales as $S = c\ln(l)/3$ with the subregion size l[1,2]. Here, the central charge c provides a universal number, which furthermore also relates to the number of degrees of freedom, e.g., for bosonic free theories. For higher-dimensional quantum systems, similar universal contributions to the entanglement entropy scaling require to consider corrections beyond the leading scaling form, which in most generic cases is set by the "area-law" scaling of the entanglement entropy S with the extend of the boundary that separates a subregion from the rest of the system[3–5]. For two-dimensional systems, on which we shall focus here, this leading asymptotic behavior reads $S = al$, in terms of the length l of the subregion's boundary, with a non-universal area-law prefactor a that depends explicitly on microscopic details of the system under consideration.

Several distinct contributions to the subleading scaling of S with l have been considered recently, related, e.g., to topological order[6,7] or the presence of Goldstone modes[8–10]. Here, we consider in particular the case of a quantum critical many-body system. For this case, there has been obtained a growing body of evidence from both numerical studies of various quantum many-body lattice models, as well as field-theoretical calculations in the continuum limit, that an isolated corner in the subregion boundary adds a logarithmic contribution, i.e., a term $c_c(\theta)\ln(l)$, to the bipartite entanglement entropy[11–23]. In order to obtain a lattice regularized version of such corner terms without introducing further lattice artifacts, boundaries with $\theta = 90°$ corners may be most conveniently considered in numerical studies on finite square lattices. On a more quantitative level, these calculations provide strong evidence that the prefactor $c_c(\theta)$ for a corner with opening angle θ to a high precision scales at least in leading order proportional to the number of field components N of the critical O(N) theory, with a prefactor that appears to be a universal function of θ for all critical ϕ^4-theory cases considered thus far.

While for the cases of $N = 1$ and $N = 3$, support for this observation has been provided by series and numerical linked cluster expansions, as well as by quantum Monte Carlo simulations,[15,16,18–21] the case of $N = 2$ has thus far not been addressed by quantum Monte Carlo studies. Here, we complement recent results from series expansion and numerical linked cluster studies[21,22] on several two-dimensional lattice models with O(2) symmetry by a quantum Monte Carlo estimate of the $\theta = 90°$ corner term. In particular, we consider the case of the quantum critical spin-half XY model on the square lattice bilayer, which provides a basic model for probing the entanglement properties at a quantum critical point with an $O(2)$ critical theory. For this model, we provide estimates for both the leading area-law prefactor a as well as the corner term $c_c(90°)$, based on the second ($\alpha = 2$) Rényi[24] entropy-based bipartite entanglement measure

$$S_\alpha(A) = \frac{1}{1-\alpha}\ln \mathrm{Tr}[(\rho_A)^\alpha], \tag{1}$$

where ρ_A denotes the reduced density matrix of the subregion (denoted A). In addition, we also consider the quantum critical spin-half XY model a the square necklace lattice (or incomplete bilayer), with in contrast to the bilayer model has a finite spin exchange interaction within only one of the two layers. We introduce both these models and locate their quantum critical points based directly on their magnetic properties in the following Sec. II. This also allows us to confirm the expected

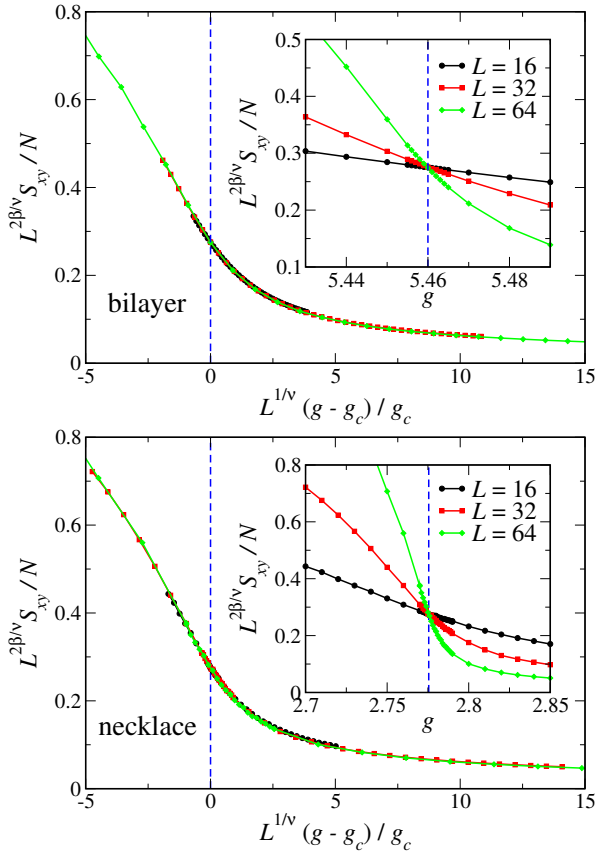

FIG. 1. (Color online) Data collapse plot of the transverse staggered spin structure factor S_{xy} within the quantum critical region of the bilayer (top panel) and the necklace (lower panel) mode. The insets show the rescaled transverse staggered spin structure factor as a function of g. Dashed lines indicate the quantum critical points. Error bars in this figure are below the symbol size.

critical exponents from a finite-size scaling analysis. In Sec. III, we then present our computational scheme and extract the entanglement entropy scaling coefficients for S_2 for both these models. These values are finally discussed in comparison to previous results in Sec. IV.

II. QUANTUM CRITICAL POINT

We consider in the following the spin-half XY-model on the square-lattice bilayer, described by the Hamiltonian

$$H = J \sum_{\langle i,j \rangle} \sum_{l=1}^{2} \left(S^x_{i,l} S^x_{j,l} + S^y_{i,l} S^y_{j,l} \right) + J_\perp \sum_i \left(S^x_{i,1} S^x_{i,2} + S^y_{i,1} S^y_{i,2} \right), \quad (2)$$

where i denotes the i-th unit cell containing two spin-half degrees of freedom (associated to the two layers, $l = 1, 2$), and J ($J_\perp$) the intra-layer (inter-layer) exchange interaction.

In addition, we consider the spin-half XY-model on the square necklace lattice (or incomplete bilayer), described by the Hamiltonian

$$H = J \sum_{\langle i,j \rangle} \left(S^x_{i,1} S^x_{j,1} + S^y_{i,1} S^y_{j,1} \right) + J_\perp \sum_i \left(S^x_{i,1} S^x_{i,2} + S^y_{i,1} S^y_{i,2} \right), \quad (3)$$

in which the inter-layer coupling has been turned to zero in one of the layers. This corresponds to a square lattice spin system with a local impurity spin attached to each lattice site, i.e. a Kondo necklace-like model with XY exchange interactions. The SU(2)-symmetric version of this model has been considered previously using quantum Monte Carlo methods, both with respect to ground state properties[25] and at finite temperatures[26]. In the following, we denote by $g = J_\perp/J$ the ratio of the inter-layer to the intra-layer exchange interactions for both models considered here.

Both models exhibits a quantum phase transition at a critical coupling ratio $g = g_c$ between a low-g phase with long-range transverse antiferromagnetic order to a large-g quantum disordered phase. The structure factor corresponding to the order parameter for this transition is given in terms of the transverse spin correlations as

$$S_{xy} = \frac{1}{N} \sum_{i,j=1}^{N} \epsilon_i \epsilon_j \langle S^x_i S^x_j + S^y_i S^y_j \rangle. \quad (4)$$

Here, the summations are performed over all spins on the finite lattice, where $\epsilon_i = \pm 1$, depending on the sublattice to which spin i belongs on the bipartite lattices. We consider in particular finite lattices of linear extend L, containing $N = 2L^2$ spins, employing periodic boundary conditions in both lattice directions. For $g < g_c$, S_{xy}/N extrapolates to a finite value in the thermodynamic limit. In Ref. 22, an estimate of $g_c = 5.460(1)$ was obtained for the bilayer model from quantum Monte Carlo simulations combined with a finite-size scaling analysis of the spin stiffness ρ_S, employing the fact that at the quantum critical point, ρ_S scales linear with L, reflecting a dynamical critical exponent $z = 1$. Here, we confirm this value of g_c from calculations of the structure factor S_{xy}, which allows us to verify explicitly also that the quantum critical behavior is indeed in accord with the expected three-dimensional $O(2)$ universality class. For this purpose, we performed quantum Monte Carlo simulations employing the stochastic series expansion approach[27] for finite lattices with periodic boundary conditions, scaling the inverse temperature $1/T = 4L$ with the linear system size in order to probe ground state correlations. Near the quantum critical point, the finite-size data exhibits conventional finite-size scaling behavior,

$$S_{xy}/N = L^{-2\beta/\nu} G(L^{1/\nu}(g - g_c)/g_c), \quad (5)$$

with a scaling function G and critical exponents β and ν, that for the three-dimensional $O(2)$ universality class

take on the values $\beta = 0.3486(1)$ and $\nu = 0.6717(1)$, respectively[28]. When performing simulations within the critical region, the above scaling form implies a common crossing point of the various finite-size values of the rescaled structure factor $L^{2\beta/\nu}S_{xy}/N$ at the quantum critical point, i.e. for $g = g_c$. This fact allows us to locate the quantum critical point as shown in the upper inset of Fig. 1. We obtain a value of $g_c = 5.460(1)$, in agreement with the previous estimate, based on the spin stiffness[22]. Furthermore, the finite size data exhibits an excellent data-collapse, confirming again the extracted value of g_c as well as the employed critical exponents of the three-dimensional $O(2)$ universality class, cf. the main upper panel of Fig. 1.

We are not aware of any previous estimate of the location of the quantum critical point for the XY necklace model, and thus performed a similar finite-size analysis as for the XY bilayer model, with the resulting data-collapse and crossing plots shown in the lower panel of Fig. 1. From our analysis, we obtain as estimate of $g_c = 2.7755(5)$ for the XY necklace model, and again find excellent accord of the numerical data with the anticipated three-dimensional $O(2)$ universality class.

III. ENTANGLEMENT SCALING

After having established the value of the quantum critical coupling ratios and confirming the three-dimensional $O(2)$ universality class of the quantum phase transitions on both lattice geometries, we next performed quantum Monte Carlo simulations to extract the scaling properties of the second Rényi entroy S_2 at these quantum critical points. In order to separate the logarithmic contribution arising from corners in the subregion boundary, we considered in each case two differently shaped subregion types, similarly to our procedure for the SU(2)-symmetric Heisenberg bilayer case[20]. First, we consider a bipartition of the toroidal simulation cell into two equally sized cylindrical strips, both of size $L/2 \times L$. The circumference of the subregion boundary in this case equals $l = 2L$. The strip-like subregions exhibit smooth boundaries without any corners. In order to introduce corners into the finite discrete-lattice subregion boundary in a controlled, scalable way, we considered in addition the case of a square subregion of size $L/2 \times L/2$, introducing this way four 90° corners along the subregion boundary. Upon increasing the linear system size L, we thus scaled the subregion size in both cases such that the aspect-ratio remained at a constant value. Any contribution to S_2 that depends only on the aspect-ratio thus reduces for both considered subregions to a l-independent, constant term. We refer to Refs.[16,17] for a discussion of various proposed functional forms of such aspect-ratio contributions to the entanglement entropy. For both subregion types, we then calculated S_2 for various boundary lengths l, employing the extended ensemble sampling approach, based on the replica trick[29,30] within the stochastic series expansion quantum Monte Carlo representation of Ref 31. We furthermore used the "increment trick"[29,31] to successively obtain the entanglement entropy upon growing the subregion for an efficient sampling.

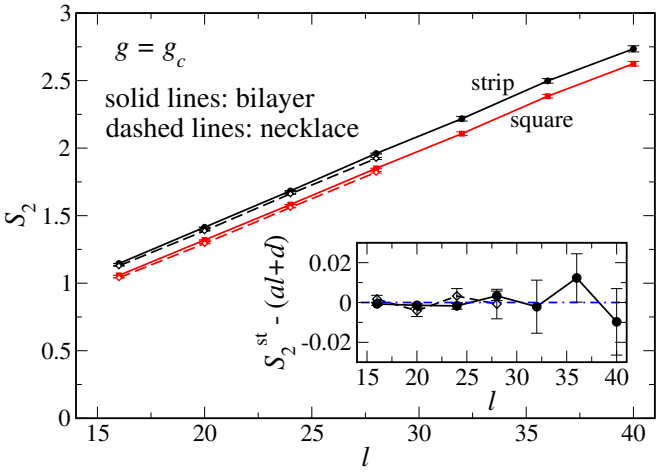

FIG. 2. (Color online) Second Rényi entropy S_2 as a function of the subregion boundary length l at the critical coupling ratio $g = g_c$ for strip and square shaped subregions. The inset shows the residuals to a linear fit $al + d$ of $S_2^{\rm st}$ for strip (st) shaped subregions boundary length l.

The results for the boundary length dependence of the entanglement entropy S_2 at the quantum critical point for both subregion types are shown in Fig. 2 for both the bilayer and the necklace lattice. We find that in both cases, S_2 exhibits a dominant area-law scaling. We first considered the case of the XY bilayer model, for which we considered system sizes from $L = 8$ to $L = 20$, corresponding to boundary lenghs between $l = 16$ and $l = 40$, respectively. As shown in the insets of Fig. 2, the strip subregion data is well accounted for by the area-law. From fitting the finite-size data for the strip subregions to a linear scaling form, we obtain the area-law scaling coefficient of $a = 0.0674(7)$ for the bilayer model. One notices also that the statistical uncertainty in our numerical data increases with increasing subregion size. This is due to the propagation of errors while employing the incremental procedure to access larger subregion sizes. We thus concentrated our computational resources towards the lower four system sizes, where accurate results for S_2 are more readily accessible. Therefore, we considered for the necklace model systems sizes from $L = 8$ to $L = 14$, corresponding to $l = 16$ and $l = 28$, respectively. In our simulations we found it not feasible to extent the considered system sizes to larger values of L, due to enhanced statistical uncertainties for the necklace model, presumable due to the lower values of the critical coupling strength g_c in that model. From fitting the finite-size data for the strip subregions to a linear scaling from, we obtain $a = 0.0664(4)$ for the quantum critical necklace model. While this is not significantly different from the above quoted value for the quantum critial bilayer

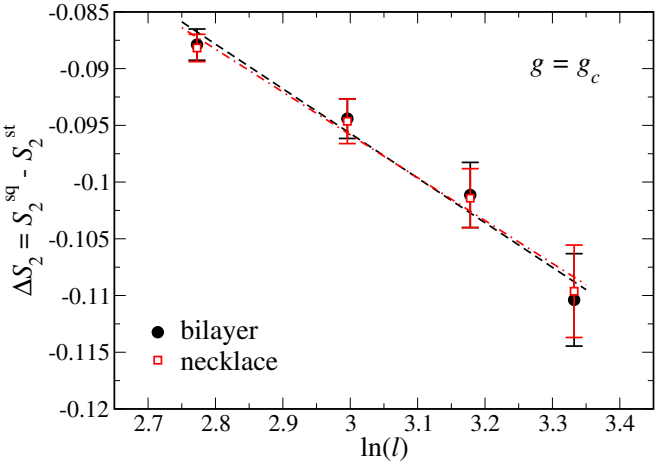

FIG. 3. (Color online) Difference between the second Rényi entropy $\Delta S_2 = S_2^{\rm sq} - S_2^{\rm st}$ for square (sq) and strip (st) subregions as a function of the subregion boundary length l (shown on a log-linear scale) at the critical coupling ratio $g = g_c$, along with the best fit line (dashed line).

model, no univeral meaning is associated to the area-law prefactor, as it depends on microscopic details.

For square subregions, we expect in addition to the leading area-law a logarithmic contribution to the entanglement scaling, due to the presence of the four corners along the subregion boundary. However, based on the finite-size data accessible to our numerical study, it is not feasible to reliably extract this logarithmic contribution from a direct fit to the square subregion data. In fact, we found that for square subregions on the restricted available l-range, the S_2 data may be fit within the statistical uncertainty also to a linear l-scaling. In order to estimate therefore the prefactor of the logarithmic term due to the presence of the four corners in the square subregion, we instead followed the procedure from Ref. 20, and considered directly the difference $\Delta S_2 = S_2^{\rm sq} - S_2^{\rm st}$ between the second Rényi entropies for the square (sq) and strip (st) subregions. This quantity is directly accessible within the quantum Monte Carlo simulations, using the fact that $\Delta S_2 = S_2^{sq} - S_2^{st} = -\ln(Z[A^{\rm sq},2,T]/Z^2) + \ln(Z[A^{\rm st},2,T]/Z^2) = -\ln(Z[A^{\rm sq},2,T]/Z[A^{\rm st},2,T])$, where Z denotes the thermal partition function of the total lattice system, and $Z[A,2,T]$ the replica-trick ensemble partition function[31] for subregions $A = A^{\rm st}$ or $A^{\rm sq}$, respectively. Our data for ΔS_2 for both the bilayer and necklace model is shown in Fig. 3 as a function of $\ln(l)$ for the lower four system sizes. While the data still exhibits statistical uncertainties, it fits well for both models to a linear dependence $\Delta S_2 = 4 \times c_{\rm c}(90^\circ)\ln(l) + \Delta d$. The resulting value of $4 \times c_{\rm c}(90^\circ) = -0.039(7)$ for the bilayer model implies a contribution to the logarithmic entanglement scaling of S_2 of $c_{\rm c}(90^\circ) = -0.010(2)$ for each 90° corner for the bilayer model, while for the necklace lattice model, we obtain values of $4 \times c_{\rm c}(90^\circ) = -0.037(7)$, and $c_{\rm c}(90^\circ) = -0.009(2)$, respectively. Both values of $c_{\rm c}(90^\circ)$ compare rather well among each other, in accord with the expectation, that the corner contribution to the entanglement scaling exhibits a universal character. It should be noted that the above error bars on the fitting parameters account for the statistical uncertainties in our quantum Monte Carlo data, but do not reflect possible systematic deviations due to further sub-leading finite-size corrections in the l-scaling of the entanglement entropy (cf. also our previous discussion in Ref. 20).

IV. DISCUSSION

Based on quantum Monte Carlo calculations of the transverse spin correlations, we identified the quantum critical points of the spin-half XY model on the square lattice bilayer and necklace lattice. Our result for the critical coupling ratio for the bilayer model agrees with a previous estimate based on the spin stiffness and furthermore exhibits finite-size scaling in accord with a three-dimensional O(2) critical ϕ^4-theory universality class, as does our finite-size data for the necklace model. At the quantum critical points, we extracted the scaling prefactors of the dominant area-law in the second Rényi bipartite entanglement entropy, as well as the additional logarithmic term from 90° corners in the subregion boundary, with consistent values for the two different models. Our results for the scaling prefactor furthermore compare well to a recent estimate of $c_{\rm c}(90^\circ) = -0.0111(1)$ from numerical linked cluster calculations[22], obtained for various two-dimensional O(2) quantum critical spin systems. They are also consistent within the statistical uncertainty with the values of $-0.0125(6)$ and $-0.0127(13)$, reported from series expansions[21]. Given that the employed computational approaches access this contribution through a rather different analysis (finite systems (here) vs. thermodynamic-limit linked-cluster calculations), we consider our results to add further support for a possible universal character of such corner terms in the bipartite entanglement measure. For the future, it will be important to apply similar methods also to quantum phase transitions that reside outside the conventional ϕ^4-theory framework, e.g. the XY* universality class[32,33], accessible in specifically designed quantum many-body systems[34].

We acknowledge discussions with P. Bröcker, T. Grover, D. J. Luitz, R. G. Melko, R. R. P. Singh, and E. M. Stoudenmire. Financial support by the Deutsche Forschungsgemeinschaft under Grant WE 3649/3-1 is acknowledged, as well as the allocation of CPU time within JARA-HPC at JSC Jülich and at RWTH Aachen University. J.H. thankfully acknowledges support from the Bonn-Cologne Graduate School for Physics and Astronomy. S.W. thanks the KITP Santa Barbara for hospitality during the program "Entanglement in Strongly-

Correlated Quantum Matter". This research was supported in part by the National Science Foundation under Grant No. NSF PHY11-25915.

[1] C. Holzhey, F. Larsen, and F. Wilczek, Nucl. Phys. B **424**, 443 (1994).
[2] P. Calabrese and J. Cardy, J. Stat. Mech.: Theor. Exp. 2004, P06002 (2004).
[3] L. Bombelli, R. K. Koul, J. Lee and R. D. Sorkin, Phys. Rev. D **34**, 373 (1986).
[4] M. Srednicki, Phys. Rev. Lett. **71**, 666 (1993).
[5] J. Eisert, M. Cramer, and M. B. Plenio, Rev. Mod. Phys. **82**, 277 (2008).
[6] A. Kitaev and J. Preskill, Phys. Rev. Lett. **96**, 110404 (2006).
[7] M. Levin and X.-G. Wen, Phys. Rev. Lett. **96**, 110405 (2006).
[8] A. B. Kallin, M. B. Hastings, R. G. Melko, and R. R. P. Singh, Phys. Rev. B **84**, 165134 (2011).
[9] M. A. Metlitski and T. Grover, arXiv:1112.5166 (2011).
[10] B. Kulchytskyy, C. M. Herdman, S. Inglis, R. G. Melko, arXiv:1502.01722 (2015).
[11] E. Ardonne, P. Fendley, and E. Fradkin, Ann. Phys. **310**, 493 (2004).
[12] E. Fradkin and J. E. Moore, Phys. Rev. Lett. **97**, 050404 (2006).
[13] H. Casini and M. Huerta, Nucl. Phys. B **764**, 183 (2007).
[14] T. Hirata and T. Takayanagi, Journal of High Energy Physics **2007**, 042 (2007).
[15] R. R. P. Singh, R. G. Melko and J. Oitmaa, Phys. Rev. B **86**, 075106 (2012).
[16] S. Inglis and R. G. Melko, New J. Phys. **15**, 073048 (2013).
[17] N. Laflorencie, D. J. Luitz, F. Alet, arXiv:1506.03703 (2015).
[18] A. B. Kallin, K. Hyatt, R. R. P Singh, and R. G. Melko, Phys. Rev. Lett. **110**, 135702 (2013).
[19] A. B. Kallin, E. M. Stoudenmire, P. Fendley, R. R. P. Singh, and R. G. Melko, Journal of Statistical Mechanics: Theory and Experiment **2014**, P06009 (2014).
[20] J. Helmes and S. Wessel, Phys. Rev. B **89**, 245120 (2014).
[21] T. Devakul and R. R. P. Singh, Phys. Rev. B **90**, 064424 (2014).
[22] E.M. Stoudenmire, P. Gustainis, R. Johal, S. Wessel, and R. G. Melko, Phys. Rev. B **90**, 235106 (2014).
[23] P. Bueno, R. C. Myers, W. Witczak-Krempa, Phys. Rev. Lett. **115**, 021602 (2015).
[24] A. Rényi, Proc. 4th Berkeley Symp. on Mathematics, Statistics and Probability **1960**, 547 (1961).
[25] L. Wang, K. S. D. Beach, A. W. Sandvik, Phys. Rev. B **73**, 014431 (2006).
[26] W. Brenig, Phys. Rev. B **73**, 104450 (2006).
[27] A. W. Sandvik, Phys. Rev. B **59**, R14157 (1999).
[28] M. Campostrini, M. Hasenbusch, A. Pelissetto, and E. Vicari, Phys. Rev. B **74**, 144506 (2006).
[29] M B. Hastings, I. González, A. B. Kallin, and R. G. Melko, Phys. Rev. Lett. **104**, 157201 (2010).
[30] R. G. Melko, A. B. Kallin, and M. B. Hastings, Phys. Rev. B **82**, 100409 (2010).
[31] S. Humeniuk and T. Roscilde, Phys. Rev. B **86**, 235116 (2012).
[32] T. Senthil, O. Motrunich, Phys. Rev. B **66**, 205104 (2002).
[33] T. Grover, A. M. Turner, and A. Vishwanath, Phys. Rev. B **84**, 195120 (2011).
[34] S. V. Isakov, R. G. Melko, M. B. Hastings, Science **335**, 193 (2012).